Surface & Coatings Technology 304 (2016) 23–30

Contents lists available at ScienceDirect

Surface & Coatings Technology

journal homepage: www.elsevier.com/locate/surfcoat

Molecular dynamics study of the growth of crystalline ZrO_2

Jiri Houska

Department of Physics and NTIS - European Centre of Excellence, University of West Bohemia, Univerzitni 8, 306 14 Plzen, Czech Republic

ARTICLE INFO

Article history:
Received 4 March 2016
Revised 28 June 2016
Accepted in revised form 1 July 2016
Available online 04 July 2016

Keywords:
Crystal growth
Ion-assisted deposition
Molecular dynamics
ZrO_2

ABSTRACT

Thin films of ZrO_2 are of high interest due to a wide range of useful technological properties. Previously, the plasma-assisted preparation of ZrO_2 has been described in terms of extrinsic process parameters such as total pressure, oxygen partial pressure or discharge power. In this paper the growth of ZrO_2 is studied by atom-by-atom molecular dynamics simulations, focused on intrinsic process parameters such as the energy and energy distribution function of arriving atoms. The results show how do the film densification, crystal nucleation and uninterrupted crystal growth depend not only on the energy delivered into the growing films (i) per fast atom (ion) or (ii) per any atom, but especially (iii) on the fraction of fast atoms in the particle flux and (iv) on the mass of fast atoms (Zr or O). In parallel, there is a clear effect of the temperature on crystal nucleation, contrary to a very weak effect of the temperature on crystal growth. The results facilitate defining new synthesis pathways for ZrO_2, and constitute phenomena which may be relevant for other coating materials (isostructural HfO_2 at the first place) as well.

1. Introduction

ZrO_2 (by far the most investigated and used ZrO_x composition) is a technologically important and cost-effective coating material [1–10]. ZrO_2 properties, ranging from good mechanical properties (hardness up to at least 17 GPa [8], effective Young's modulus up to at least 166 GPa [9]) and excellent thermal stability (melting point of 2860 °C) through high refractive index (at 550 nm up to at least 2.22 [8]) and ionic conductivity [1] to high dielectric constant (up to at least 22 [10]), lead to numerous applications such as diffusion and thermal barriers, ionic conductors, interference optical filters or high-k dielectrics in microelectronics. Furthermore, many of the ZrO_2 properties and applications, and arguably also phenomena related to its structure formation, are shared by equally important isostructural HfO_2 [11–18]. Crystalline phases of ZrO_2, ordered by increasing density and experimental interest, include monoclinic, tetragonal and cubic (m-, t- and c-ZrO_2, respectively). An important quantity to note is the Zr coordination (N_{Zr}) which is slightly below 7 in amorphous a-ZrO_2 [19] ("intrinsically preferred" value given by the size of Zr and O atoms), 7 in m-ZrO_2 and 8 in t- and c-ZrO_2. Consequently, the low-density m-ZrO_2 phase is relatively easy to prepare because it is characterized by (almost) preferred N_{Zr}, contrary to the "overcoordinated" t- and c-ZrO_2.

Ion-assisted deposition techniques constitute a common method of ZrO_2 fabrication, and a large experimental and theoretical effort is being devoted to investigating the relationships between deposition conditions and the resulting material structure and properties. Preparation and stabilization of high-density t- and c-ZrO_2 is an important part of these efforts. On the one hand, ZrO_2 thin films covering a wide range of characteristics can be prepared by varying extrinsic process parameters such as sputtering power [8], substrate bias voltage, substrate heating [4], discharge gas pressure and composition [2,3,6,7] or duty cycle and frequency (in case of pulsed discharges) [8]. (Let alone the stabilization of the high-density phases by Y [7] or by O vacancies [20].) On the other hand, the film growth is in fact controlled by intrinsic process parameters such as the particle flux composition, ion fraction in the particle flux, ion energy and surface temperature (affected by both the ohmic heating and the ion bombardment). The intrinsic parameters of course depend on the extrinsic ones, but are much more difficult both to directly adjust and to measure.

An important thing to note in this context is that the typical time scale of film growth (10^{-1} s per monolayer) is many orders of magnitude longer than the time scale of bond-breaking and bond-forming processes, thermal spike cooling and structure formation ($<10^{-12}$ s in the case of homogenous materials [21] and $\leq 10^{-9}$ s in the case of nanocomposites due to longer required diffusion lengths [22]). Thus, each particle impact, ranging from slow neutrals to the most energetic (hundreds eV) ions, has to be considered separately (instead of averaging the energy over all particles) for many purposes. Note that the energetic particles are present (and important [23]) not only (i) due to the negative substrate bias but also due to the (ii) reflection from the sputter target, (iii) acceleration of negative (typically oxygen) ions from the target [24] and (iv) high-energy tails of sputtered atoms (particularly at high sputtering powers). Furthermore, the atomic-scale processes may depend not only on the energy but also on the momentum delivered by the particle impact (i.e. on the particle mass) [25].

E-mail address: jhouska@kfy.zcu.cz.

http://dx.doi.org/10.1016/j.surfcoat.2016.07.004

Currently there is no work dealing with a physics-based description of the growth of ZrO_2 during ion bombardment. Consequently, there is little quantitative information about the complex relationships between the intrinsic process parameters and the atomic-scale processes that under various conditions may or may not lead to ZrO_2 nucleation and to uninterrupted growth or amorphization of ZrO_2 crystals. While ab-initio simulation can and did reveal numerous characteristics of ZrO_2 [26,27] and ZrO_x [28], they cannot capture the aforementioned processes because of computational costs. Classical (empirical potentials-based) molecular dynamics (MD) simulations are suitable for reproducing such processes and can provide information not accessible experimentally. Their significant advantage is a disentanglement of processes which happen in parallel in the experiment (crystal nucleation and crystal growth, arriving of low- and high-energy particles, ohmic heating and heating of the film surface by ions, etc.). MD simulations were successfully used to describe the growth of C [29], Si [30], SiC [31], SiNH [32], SiO_2 [33], MgAlO [34], TiO_2 [35] or Al_2O_3 [36] (Ref. [36] also includes a more detailed overview). MD simulations of ZrO_2 radiation damage (albeit based on the interaction potential not recommended for simulations of ZrO_2 growth [37]) can be found in Ref. [38].

In this work, the growth of c-ZrO_2 (the most desired phase) is systematically investigated in a wide range of process parameters by MD simulations. The parameters of interest include (i) fraction of fast atoms in the total particle flux (f_{fast}), (ii) energy of the fast atoms (E), (iii) mass of the fast atoms (i.e. whether the energy is delivered by Zr or by O), (iv) growth temperature (T) and (v) growth template (c-ZrO_2 (001) or a-ZrO_2). The aim is to provide quantitative information for the ZrO_2 case, to provide qualitative information relevant for similar materials, and to examine the possibility to capture not only crystal growth but also crystal nucleation (rarely studied using this technique).

2. Methodology

All simulations were performed using the LAMMPS [39] code. The film growth simulations were performed using periodic boundaries in horizontal directions, and a vacuum slab in the vertical direction. The recursive simulation protocol includes:

(1) generation of a growth template (600 atoms of c- or a-ZrO_2 including a frozen bottom layer; horizontal size 5× lattice constant = 2.543 nm) and a 1 ps long “thermalization run” (canonical ensemble) at $T = 300$, 400, 500, 600, 700 or 800 K (Nose-Hoover thermostat);
(2) generation of 3 new isolated atoms above the film surface, with velocities (towards the surface) corresponding to $E = 0.1$–400 eV (fast atoms) or 0.1 eV (slow atoms).
(3) a 5 ps long “collisional run” without controlling the temperature of film atoms (microcanonical ensemble) but at a continuing temperature control of the original substrate atoms, in order to simulate particle collisions and energy dissipation;
(4) a 1 ps long “thermalization run” (canonical ensemble) at the temperature T, in order to reestablish the deposition temperature;
(5) removal of resputtered (desorbed) atoms and a return to (2).

The growth template can represent not only a real substrate or a seed layer for an epitaxial growth, but also previously grown part of the film/previously nucleated crystal. The composition of the film-forming flux was adaptively changed (because of slightly different sticking coefficients of Zr and of O for some E values) in order to keep the Zr/O = 1/2 composition of the films. 3000 atoms (including those not incorporated into the film and removed in the step 5) were deposited in 1000 cycles of the above algorithm. Processing of the results included calculations of N_{Zr}, performed using the Zr—O bonding distance cutoff of 2.65 Å (upper bound of the first peak of Zr—O radial distribution functions).

It is well known that the interaction potential choice is critical for the success and reliability of classical MD simulations. For example, the fact that the crystal phase of interest constitutes an energy minimum does not automatically guarantee that the corresponding interaction potential can be successfully used for simulations of the nonequilibrium open surface growth. Simulations in this work use the partial-charge ($Zr^{+3.542}$, $O^{-1.771}$) Buckingham-type ($U = Ae^{-r/\rho} - Cr^{-6}$) potential fitted in Ref. [37]. While all the relevant details and considerations are described in Ref. [37], the main feature of the potential used (Fig. 1) is the following. On the one hand, the full-charge (Zr charge $q_{Zr} = 4e$) potentials available in older literature yield too low preferred $N_{Zr} \leq 6$. Consequently, ZrO_2 growth simulations using such potentials lead to a formation of fictitious rutile-like structure characterized by $N_{Zr} = 6$ (left panel of Fig. 1). On the other hand, decreasing q_{Zr} (switching from full charge to partial charge potentials; changing the short-range parameters in parallel in order to preserve the ground state lattice constant and energy) leads to increasing preferred N_{Zr}, e.g. to $N_{Zr} = 7$ for the potential recommended in Ref. [37] and used in this work ($q_{Zr} = 3.542e$). Growth simulations using q_{Zr} around this optimum value can lead (at proper E) to uninterrupted c-ZrO_2 growth (middle panels of Fig. 1). It is also worth to mention a limitation resulting from the fixed non-zero elemental charges: the simulations do not describe dissociation of O_2 molecules on the film surface. However, due to the low O_2 sticking coefficient this was not considered to be critical for the conclusions made.

3. Results and discussion

The results are presented as follows. First, the effect of E (Figs. 2–3) and energy distribution function (EDF, Figs. 4–7) on the epitaxial growth of c-ZrO_2 on c-ZrO_2 is presented in Sections 3.1 and 3.2, respectively. Because no systematic effect of T on the growth was observed, the graphical results are shown for $T = 300$ K only and the numerical results are shown as averages over the aforementioned six T values. Next, the effect of E and EDF on the nucleation and growth of c-ZrO_2 on a-ZrO_2 (Figs. 8–10) is presented in the same way in Section 3.3. Finally, the effect of T on the nucleation (Figs. 11–12) is presented in Section 3.4.

3.1. Effect of energy

Fig. 2 shows structures grown on c-ZrO_2 as a function of E. First, increasing E leads to materials densification (decreasing volume of nanopores). Note that the formation of nanopores was observed only in the crystalline films (not in the amorphous films studied below). This indicates the mechanism of the formation of nanopores: the low-energy atoms first form a low-density amorphous network on the film surface, and then move to the crystalline positions due to the epitaxial growth (the low-density amorphous surface “segregates” to high-

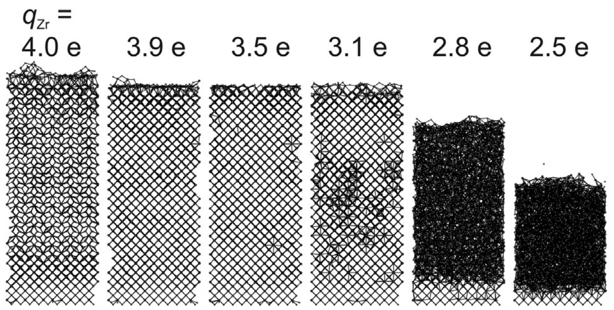

Fig. 1. Examples of ZrO_2 (600 substrate atoms + 3000 film atoms) grown on c-ZrO_2 at $E = 100$ eV using different Buckingham interaction potentials defined by different elemental charges (q_{Zr} and $q_O = -0.5 \times q_{Zr}$) [37].